Photoelectric absorption as an x-ray spectral diagnostic of massive star winds

Erin Martell,[1] Emma Wollman,[1] David Cohen,[1] Marc Gagné,[2] and Maurice Leutenegger[3]

1: Swarthmore College; 2:West Chester University
3: NASA/Goddard Space Flight Center

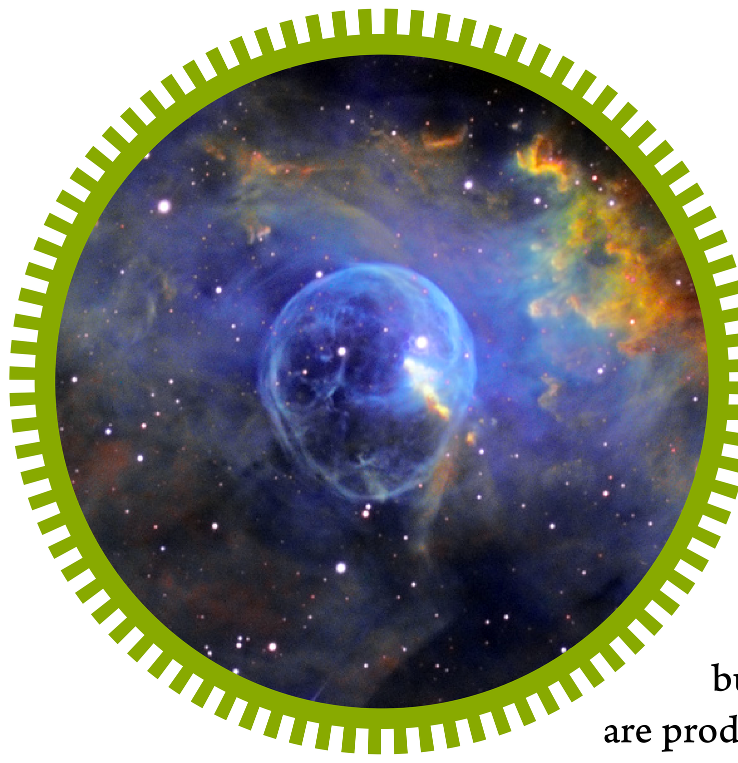

Massive star winds

The winds of massive stars deposit chemically enriched matter as well as energy and momentum into their galactic environment (wind-blown bubble NGC 7635 at left). The x-rays are produced very close to the star, however, necessitating the use of spectroscopy of the unresolved central stars in order to understand the physics that governs the energetic processes that produce the observed X-ray emission

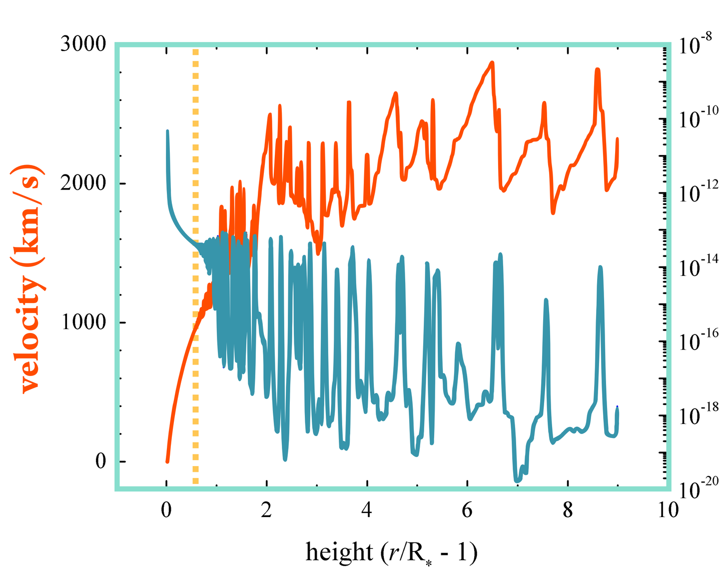

X-ray production

Instabilities lead to shock-heating of the wind. These shocked regions, which make up a small fraction of the total wind mass, reach temperatures between 10^6 and 10^7 K. In the simulation shown to the left, shocks start developing about half a stellar radius above the surface of the star.

Theoretical predictions

1. In the shock regions, highly ionized atoms produce x-ray thermal emission lines.

2. Doppler broadening due to production in the fast-moving wind results in broad lines.

3. The cool material in the wind absorbs x-rays. We should find evidence of this absorption in both the overall spectrum and in the shape of individual line profiles.

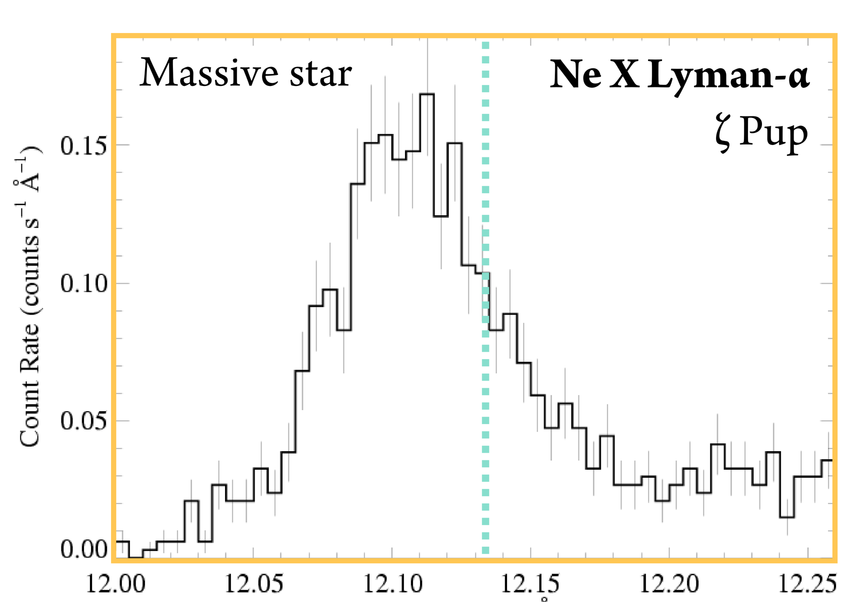

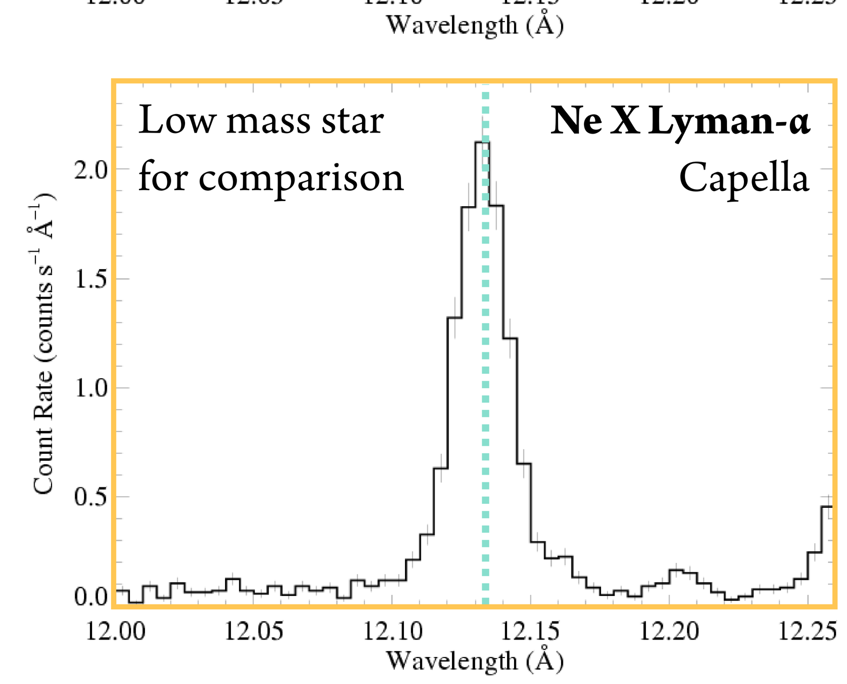

Chandra data

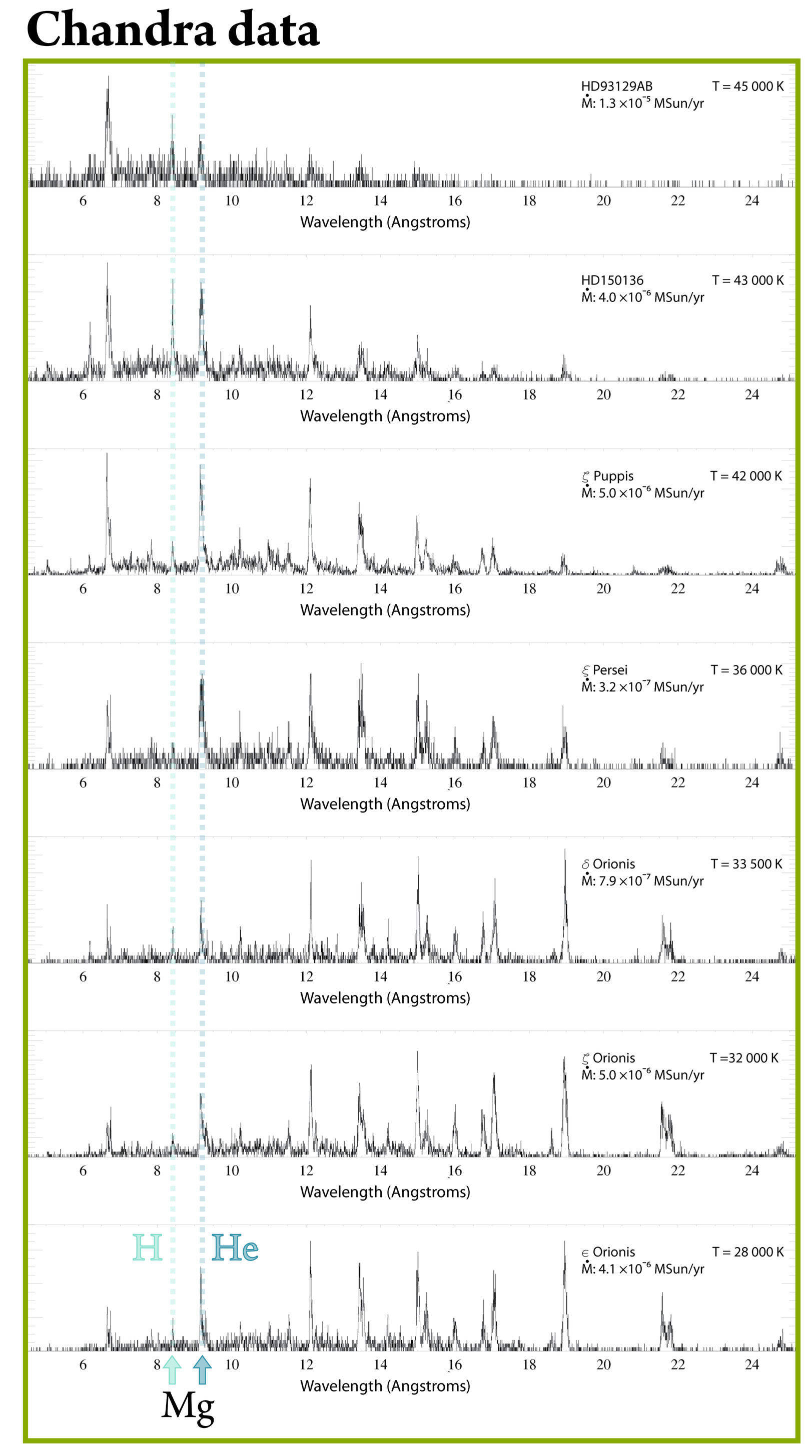

Wind absorption models

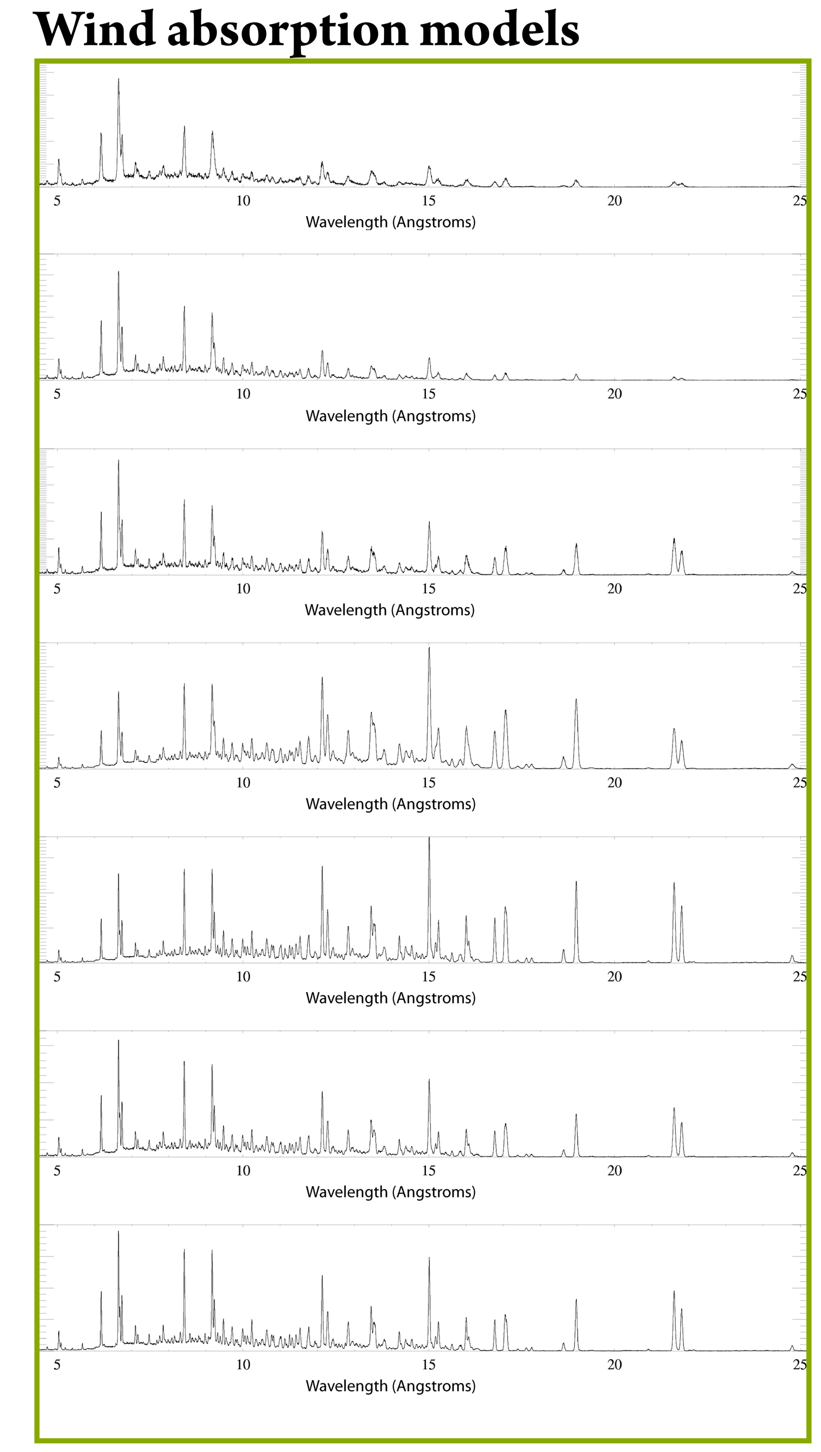

Chandra spectra of massive stars

High-resolution X-ray spectra of massive stars show a trend in spectral hardness with stellar surface temperature (and mass and luminosity): above left, hottest stars at top have hardest spectra.

Is this trend due to the emission temperature of shock-heated plasma? Or, is it due to increasing wind absorption of X-rays for hotter stars that have stronger winds?

To explore the effect of wind absorption, we have developed a radiation transport model of thermal X-ray emission from plasma embedded within an extended stellar wind. Preliminary models that all assume the same emission temperature but with differing amounts of wind attenuation (shown in the right panel) reproduce the observed hardness trend. Some residual plasma temperature emission effect may remain, however – ratios of H/He-like lines (which are not subject to significant differential absorption) are the key to determining this.

Atomic opacity

The opacity of the (cold, unshocked component of the) wind is due to K-shell photoionization of low-Z elements: C, N, O, Ne, Mg and the L-shell of Fe and Ni in a cosmic abundance mixture (O dominates).

The opacity is greater at longer wavelengths: Wind absorption hardens the overall X-ray spectrum. (Figure at top of this column.)

And this continuum opacity also skews the individual Doppler-broadened line profiles (explained in the right-hand column).

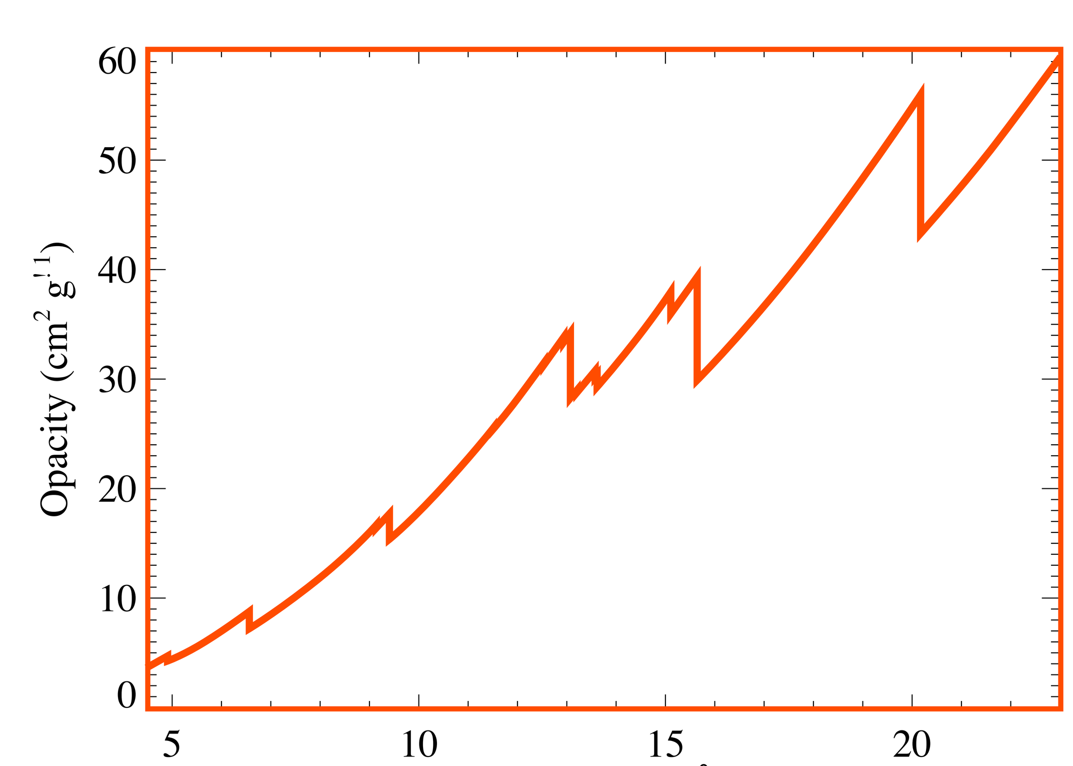

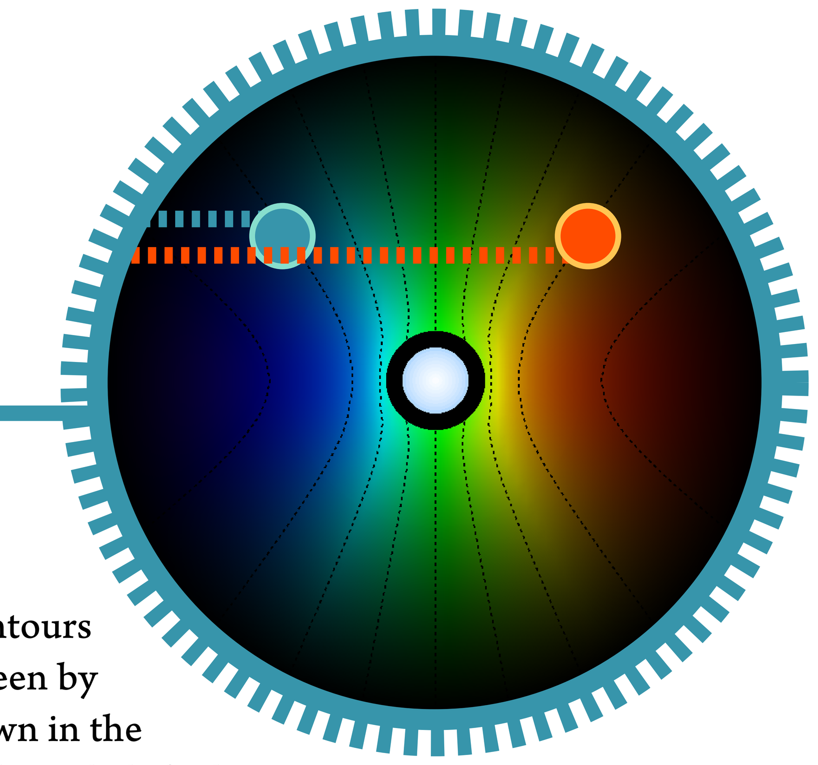

Wind geometry

The shape of the individual x-ray emission lines is also governed by absorption. The diagram to the right shows contours of constant radial velocity as seen by an observer to the left. As shown in the diagram, x-rays emitted from the red-shifted side of the wind must pass through more material than blue photons emitted from the front of the wind. Red photons are thus preferentially absorbed, leading to asymmetrical lines.

Line asymmetry

In our model of the line profile shape, the asymmetry is parameterized by τ_*, the fiducial optical depth. τ_* is defined as $\kappa \dot{M}/4\pi R_* v_\infty$, where κ is the opacity, R_* is the stellar radius, and v_∞ is the terminal velocity. Plotted to the right are four un-normalized models with different values of τ_*. The blue line has the highest τ_* value and the orange line the lowest.

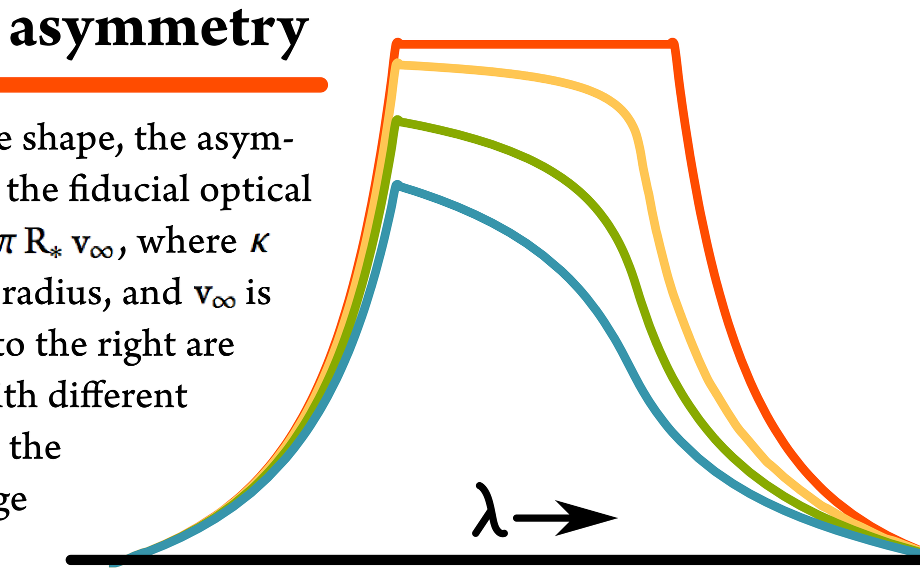

∞

Fitting the data

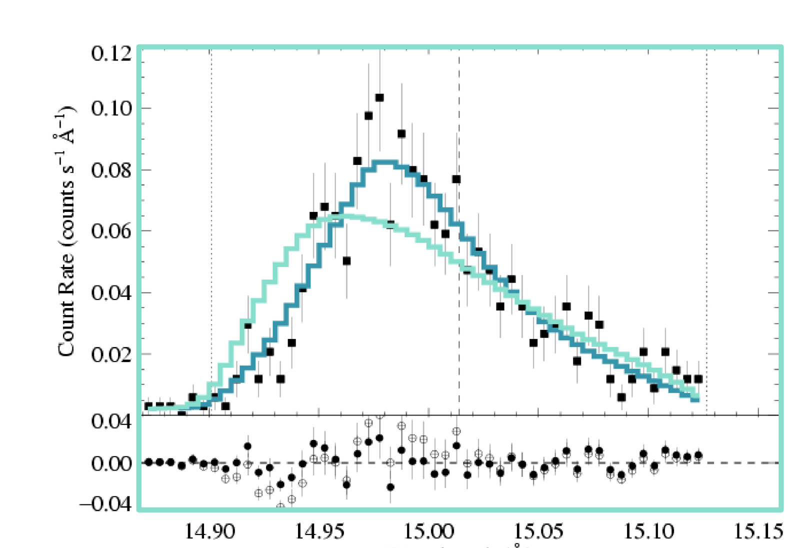

To the left, the Fe XVII line at 15.014 angstroms is shown with two models. The dark blue model represents the best fit and yields a τ_* value of 1.94. The fit also gives us the radius of x-ray emission onset, which is 0.55 stellar radii above the star's surface for this line. The light blue model represents a fit with a fixed τ_* value of 5.30 dictated by the mass-loss rate obtained from H-alpha diagnostics. The best-fit curve is clearly less shifted than predicted by the H-alpha mass-loss rate, indicating a lower mass-loss rate.

Mass-loss rate determination from global fit

The same mass-loss rate reduction can be seen when τ_* values are plotted for all lines. As we know the terminal velocity, stellar radius, and have a model of the opacity, we can fit the mass-loss rate to the data. The solid curve shows the best-fit mass-loss rate of 3.5e-6 solar masses per year and the dashed curve shows the literature mass-loss rate of 8.3e-6 solar masses per year. We see that the H-alpha mass-loss rate is inconsistent with the data and that a lower mass-loss rate is preferred. In other stars, the best fit mass-loss rates are up to an order of magnitude lower than values obtained from other diagnostics.